Journal of Organometallic Chemistry, 385 (1990) 387–398
Elsevier Sequoia S.A., Lausanne – Printed in The Netherlands
JOM 20501

Substitution chemistry of pentaosmium carbonyl clusters: crystal structure of $H_2Os_5(CO)_{13}P(OMe)_3PEt_3$

Brian F.G. Johnson, Rajesh Khattar, Jack Lewis *, Paul R. Raithby, and Maria J. Rosales *

University Chemical Laboratory, Lensfield Road, Cambridge CB2 1EW (Great Britain)

(Received September 29th, 1989)

Abstract

Thermolysis of $H_2Os_5(CO)_{14}P(OMe)_3$ with an excess of L′ (L′ = $P(OMe)_3$ or PEt_3) in toluene at 80 °C initially affords an addition product with a formulation $H_2Os_5(CO)_{14}LL'$, which undergoes decarbonylation on prolonged heating to give $H_2Os_5(CO)_{13}LL'$. The latter cluster can be obtained under much milder conditions by the direct reaction of $H_2Os_5(CO)_{14}P(OMe)_3$ with Me_3NO in the presence of the appropriate phosphorus donor ligand. A single crystal structure of $H_2Os_5(CO)_{13}P(OMe)_3PEt_3$ has revealed a trigonal bipyramidal metal framework with a $P(OMe)_3$ ligand attached to an apical osmium atom and a PEt_3 ligand attached to an equatorial osmium atom of the bipyramid. Both of the hydride ligands have been shown by potential energy calculations to be edge-bridging. In solution, these hydride ligands are fluxional at room temperature; the fluxional process can be frozen by cooling the sample to 213 K, where the ^1H NMR spectrum shows a pair of doublets of doublets.

Introduction

The substitution chemistry of the pentaosmium carbonyl clusters $H_2Os_5(CO)_{15}$ and $Os_5(CO)_{16}$ has been studied by the thermal and chemical activation of the Os–CO bond [1–4]. Thermolysis gives an addition product at the expense of a metal–metal bond [1], whereas chemical activation gives a simple substituted product [4]. For example, thermolysis of $H_2Os_5(CO)_{15}$ with $P(OMe)_3$ in refluxing octane yields an addition product $H_2Os_5(CO)_{15}P(OMe)_3$ with an open edge-bridged tetrahedral metal skeleton that undergoes decarbonylation on further heating to

* Present address: Institude De Quimica, Universidad Nácional Autonoma de México, Ciudad Universitaria, Coyoacan 04510 (D.F. Mexico).

0022-328X/90/$03.50

afford $H_2Os_5(CO)_{14}P(OMe)_3$, which has a closed trigonal bipyramidal metal skeleton [1,2]. The latter cluster can be obtained [4] directly by the chemical activation of $H_2Os_5(CO)_{15}$ with Me_3NO in the presence of $P(OMe)_3$. Recently, we showed that the decarbonylation of $H_2Os_5(CO)_{15}P(OMe)_3$ to form $H_2Os_5(CO)_{14}P(OMe)_3$ is accompanied by the metal framework reorganisation, and suggested a mechanism showing metal framework reorganisation [4].

We have investigated further the substitution of $H_2Os_5(CO)_{14}L$ by simple phosphorus donor ligands, and now describe the synthesis and crystal structure of $H_2Os_5(CO)_{13}P(OMe)_3PEt_3$ and some of its chemistry. A preliminary communication has appeared [2].

Results and discussion

Reactivity of $H_2Os_5(CO)_{14}L$

The cluster $H_2Os_5(CO)_{15}$ (**1**) reacts with a range of nucleophiles to give addition products of the type $H_2Os_5(CO)_{15}L$ ($L = P(OMe)_3$, PEt_3 or PPh_3) in which one metal–metal bond is broken and an edge-bridged tetrahedral metal framework formed [1]. The incoming ligand L has been shown by X-ray crystallography to occupy an equatorial site on the edge-bridged metal atom [1]. The complex $H_2Os_5(CO)_{15}L$ undergoes decarbonylation on further heating to give $H_2Os_5(CO)_{14}L$ ($L = P(OMe)_3$ (**2**) or PEt_3 (**3**)), which is based on a trigonal bipyramidal metal skeleton with the ligand L attached to one of the equatorial osmium atoms of the bipyramid [2]. It was therefore thought that the complex $H_2Os_5(CO)_{14}L$, which is isoelectronic with **1** and has a trigonal bipyramidal geometry, may undergo a similar kind of reaction with the ligand L to afford an addition product with an open structure. In the light of this, the thermolysis of $H_2Os_5(CO)_{14}L$ in the presence of an excess of ligand L was investigated. When **2** was treated with ligand L ($L = P(OMe)_3$ or PEt_3) in refluxing n-heptane for 16 h, the product of formula $H_2Os_5(CO)_{13}P(OMe)_3L$ ($L = P(OMe)_3$ (**4**) or PEt_3 (**5**)) was obtained. If the thermolysis is carried out in toluene at 80 °C for shorter time the product is a brown cluster with the formula $H_2Os_5(CO)_{14}P(OMe)_3L$ ($L = P(OMe)_3$ (**6**) or PEt_3 (**7**)), which undergoes decarbonylation to give **4** on further heating. The latter reaction is reversible, the reaction of **4** with CO (40 atm, 50 °C) affording mainly **6**. The clusters **6** and **7** have been characterised by IR and mass spectroscopy (see Table 1 for **6**). The ^1H NMR spectrum of **6** at room temperature in the hydride region displays a number of resonances indicative of the presence of isomers in solution and shows no change when the solution is cooled to 213 K. Attempts to grow suitable single crystals of **6** were not successful. Since **6** exists in a number of isomeric forms in solution, neither ^1H nor ^{31}P NMR spectroscopy is of great help, and we do not know the exact location of either the hydride or the phosphite ligand in this cluster. In terms of electron counting, the cluster with the formula $H_2Os_5(CO)_{14}P(OMe)_3L$ is a 74 electron species, and a square-based pyramidal or an edge-bridged tetrahedral metal framework is predicted by both the effective atomic number (e.a.n.) rule and the polyhedral skeletal electron pair theory. If the reaction of **2** with $P(OMe)_3$ proceeds by the opening out of the trigonal bipyramid, in a manner similar to that observed [1] in the formation of $H_2Os_5(CO)_{15}P(OMe)_3$, then an edge-bridged tetrahedral metal skeleton may be proposed for the cluster

Table 1

Infrared and mass spectral data for compounds **6**, **8** and **9**

Cluster	IR spectrum [a] ν(CO) (cm^{-1})	Mass spectrum [b] (m/e)
$H_2Os_5(CO)_{14}\{P(OMe)_3\}_2$ (**6**)	2093 (vw), 2055 (m), 2030 (vs), 2012 (m), 1991 (w), 1971 (w,br)	1602
$H_2Os_5(CO)_{13}\{P(OMe)_3\}_2$ (**8**)	2077 (s), 2032 (vs), 2007 (s), 1968 (m)	1574
$H_2Os_5(CO)_{13}P(OMe)_3PEt_3$ (**9**)	2077 (m), 2027 (s), 2005 (s) 1969 (m)	1570

[a] In CH_2Cl_2. [b] Based on ^{192}Os.

$H_2Os_5(CO)_{14}P(OMe)_3L$ (L = $P(OMe)_3$ (**6**) or PEt_3 (**7**)) (Fig. 1), although a square based pyramidal structure is also possible.

The conversion of $H_2Os_5(CO)_{14}P(OMe)_3$ into $H_2Os_5(CO)_{14}P(OMe)_3L$ (L = PEt_3 (**7**), structure **A**) simply involves the opening out of the cluster to accommodate the incoming ligand L, whereas the transformation to structure **B** would involve either the metal framework rearrangement or phosphite migration, or perhaps both. We have not so far been able to determine what is actually happening. A similar situation is encountered in the transformation of $H_2Os_5(CO)_{15}P(OMe)_3$ to $H_2Os_5(CO)_{14}P(OMe)_3$ [2,4]. In these case the ligand migration has been ruled out on the basis of spectroscopic data, and a metal framework rearrangement has been proposed to be occurring [4]. Metal framework rearrangement is a common feature in metal cluster chemistry, and has been observed in a number of heterometallic clusters containing Group IB metal ligands and a number of mechanisms have been proposed [5,6]. It is more likely that the transformation of $H_2Os_5(CO)_{14}P(OMe)_3$ to $H_2Os_5(CO)_{14}P(OMe)_3L$ (L = PEt_3 (**7**), structure **B**) may involve a metal framework rearrangement (if it is assumed that no phosphite migration is taking place) and is shown in Fig. 2. This rearrangement proceeds via a square-based pyramidal metal skeleton as an intermediate, which is an alternative geometry for a 74 electron species and is in accordance with Johnson's proposed mechanism [7].

On further heating in toluene at 80 °C, the cluster $H_2Os_5(CO)_{14}P(OMe)_3L$ undergoes decarbonylation to afford $H_2Os_5(CO)_{13}P(OMe)_3L$ (L = $P(OMe)_3$ (**8**) or PEt_3 (**9**)). These clusters have been fully characterised by spectroscopic techniques (Table 1). The IR spectra of **8** and **9** in the terminal carbonyl region are very similar, indicating that they have a similar structures. The ^1H NMR spectrum of **8** does not display any resonances in the hydride region at 298 K, but as the sample is cooled to 253 K, broad and weak resonances at δ −19.8 and −22.7 start to appear (Fig. 3).

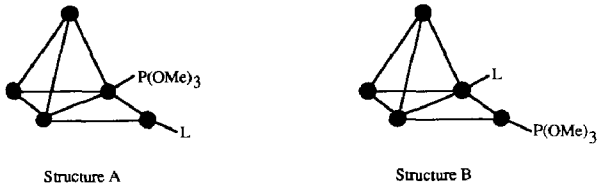

Structure A Structure B

Fig. 1. Proposed structure of $H_2Os_5(CO)_{14}P(OMe)_3L$ (L = PEt_3 (**7**)).

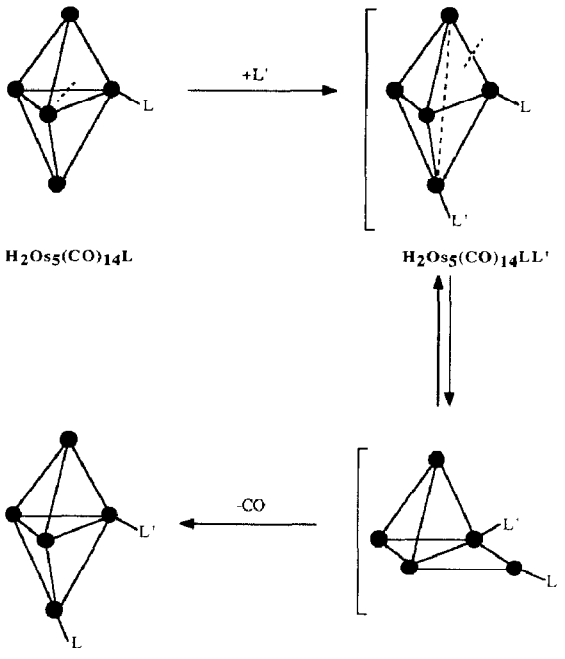

Fig. 2. Proposed mechanism for the transformation of $H_2Os_5(CO)_{14}L$ (**2**) to $H_2Os_5(CO)_{13}LL'$ (**9**) (L = $P(OMe)_3$, L' = PEt_3).

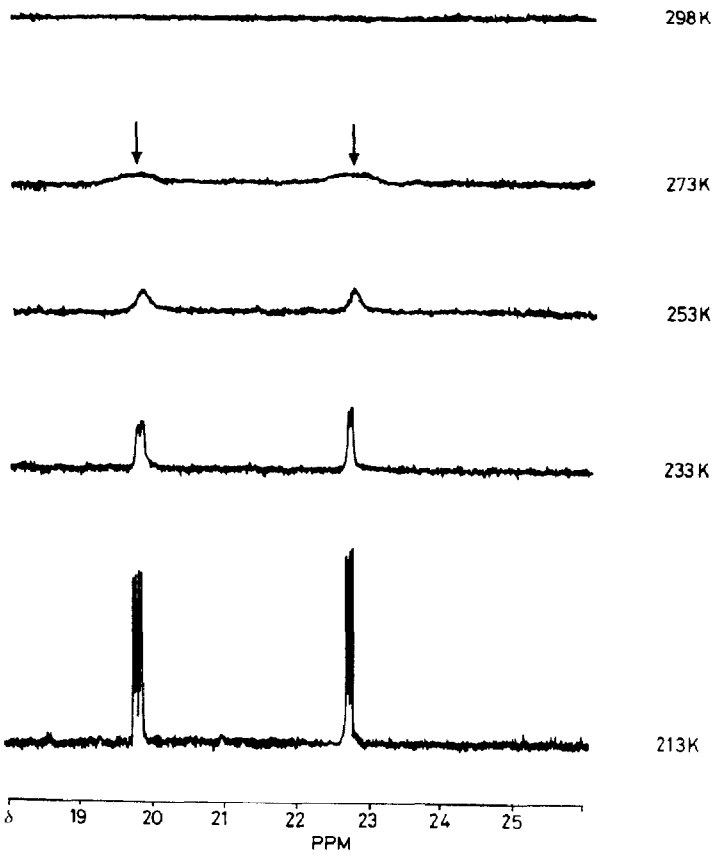

Fig. 3. ^1H NMR spectrum of $H_2Os_5(CO)_{13}\{P(OMe)_3\}_2$ (**8**) at variable temperatures.

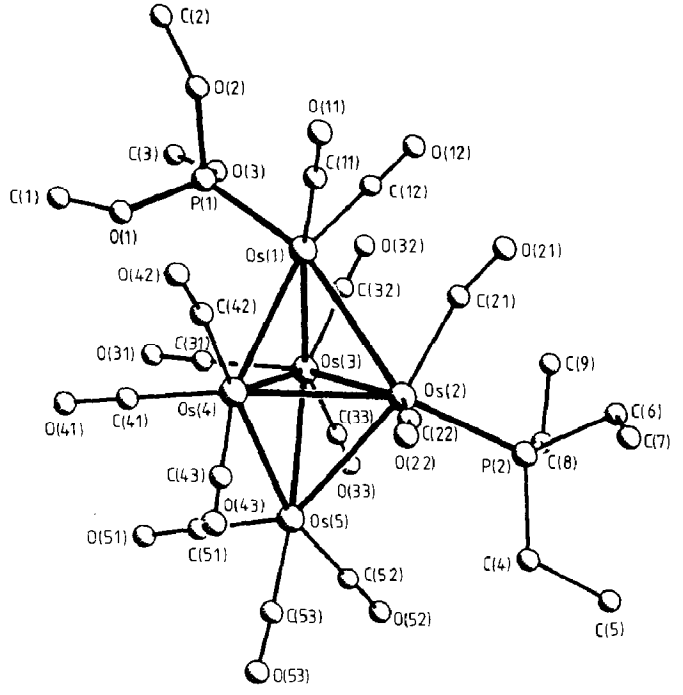

Fig. 4. The molecular structure of $H_2Os_5(CO)_{13}P(OMe)_3PEt_3$ (**9**).

On further cooling to 233 K these resonances sharpen, and finally at 213 K the spectrum exhibits a pair of doublets of doublets (Fig. 3). This suggests that both the hydride ligands are coupled to the phosphorus atom of the $P(OMe)_3$ group and are in the edge-bridging (μ_2-) positions. $^{31}P\{^1H\}$ NMR spectrum of **8** displays a pair of doublet resonances, one at δ −34.87 and another at −63.23 with $^3J(P-P)$ ca. 11 Hz, suggesting that both the phosphite ligands are in the inequivalent environment, and this is supported by the ^1H NMR spectra, which show two distinct doublet resonances with $^3J(P-H)$ ca. 12 Hz.

In terms of electron counting the cluster with formula $H_2Os_5(CO)_{13}P(OMe)_3L$ is a 72 electron species and a closo-trigonal bipyramidal metal framework is predicted by both the effective atomic number (e.a.n.) rule and the polyhedral skeletal electron pair theory. In order to confirm this prediction and also to establish the exact molecular geometry of these clusters, a single crystal X-ray structure determination was carried out for **9**. Suitable single crystals of **9** were grown by the slow evaporation of CH_2Cl_2/hexane solution at −5 °C during 3–4 days.

The molecular structure of $H_2Os_5(CO)_{13}P(OMe)_3PEt_3$ (**9**) is shown in Fig. 4. Lists of bond lengths and bond angles are given in Tables 2 and 3. The five osmium atoms define a trigonal bipyramid with a $P(OMe)_3$ ligand attached to an apical osmium atom and a PEt_3 ligand attached to an equatorial osmium atom. All the carbonyl ligands are terminally coordinated. The osmium atoms which are associated with the phosphorus donor ligands are coordinated to two terminal carbonyl ligands, whereas the remaining osmium atoms are each coordinated to three carbonyl ligands. The hydride ligands were not located directly in the crystallographic study, but have been placed at the positions shown in the Fig. 5 on the basis of potential energy calculations. Both the hydride ligands bridge the equivalent

Table 2

Bond lengths (Å) for $H_2Os_5(CO)_{13}P(OMe)_3PEt_3$ (**9**)

Os(1)–Os(2)	2.990(2)	Os(1)–Os(3)	2.879(2)
Os(1)–Os(4)	2.684(2)	Os(1)–P(1)	2.238(5)
Os(1)–C(11)	1.915(19)	Os(1)–C(12)	1.877(22)
Os(2) Os(3)	2.897(2)	Os(2)–Os(4)	2.821(2)
Os(2)–Os(5)	3.045(2)	Os(2)–P(2)	2.380(5)
Os(2)–C(21)	1.913(29)	Os(2)–C(22)	1.874(18)
Os(3)–Os(4)	2.824(2)	Os(3)–Os(5)	2.847(2)
Os(3)–C(31)	1.996(20)	Os(3)–C(32)	1.907(22)
Os(3)–C(33)	1.915(25)	Os(4)–Os(5)	2.737(2)
Os(4)–C(41)	1.913(20)	Os(4)–C(42)	1.830(24)
Os(4)–C(43)	1.903(27)	Os(5)–C(51)	1.925(20)
Os(5)–C(52)	1.913(25)	Os(5)–C(53)	1.900(24)
P(1)–O(1)	1.537(27)	P(1)–O(2)	1.629(26)
P(1)–O(3)	1.566(19)	O(1)–C(1)	1.321(48)
O(2)–C(2)	1.425(52)	O(3)–C(3)	1.343(33)
P(2)–C(4)	1.783(29)	P(2)–C(6)	1.841(22)
P(2)–C(8)	1.833(28)	C(4)–C(5)	1.572(35)
C(6)–C(7)	1.498(35)	C(8)–C(9)	1.469(55)
C(11)–O(11)	1.127(24)	C(12)–O(12)	1.178(29)
C(21)–O(21)	1.119(33)	C(22)–O(22)	1.148(24)
C(31)–O(31)	1.039(24)	C(32)–O(32)	1.135(27)
C(33)–O(33)	1.150(30)	C(41)–O(41)	1.141(24)
C(42)–O(42)	1.190(31)	C(43)–O(43)	1.146(31)
C(51)–O(51)	1.118(24)	C(52)–O(52)	1.162(30)
C(53)–O(53)	1.152(30)		

equatorial Os(2)–Os(3) and equatorial–axial Os(2)–Os(5) edges, and a similar arrangement of hydride ligands has been observed previously in the mono-substituted complex $H_2Os_5(CO)_{14}PEt_3$ (**3**) [2,4].

The structural parameters for **9** are similar to those for the mono-substituted complex **3**. Again the longest Os–Os bonds are associated with the equatorially phosphine substituted metal atom, Os(2). In this structure the apical Os(1) atom is electron-poor with 17 electrons, while one of the equatorial osmium atom is formally electron-rich. The electron imbalance is partially redressed by two incipient semi-bridging carbonyl groups, C(21)O(21) and C(42)O(42), which bridge to Os(1) (Os(1)–C(21), 2.78(3) Å; Os(2)–C(21)–O(21), 166(2)°; Os(1)–C(42), 2.63(3) Å; Os(4)–C(42)–O(42), 167(3)°). The equatorial Os(2)–P(2) phosphine distance is similar in to the equatorial Os–P phosphine distance in **3**, while the axial Os(1)–P(1) phosphite distance is ca. 0.14 Å shorter.

The hydride positions in these two structures are of particular interest. It might be expected that, in order to maintain an electronically balanced structure, each apical metal atom would be bonded to a hydride which bridges to an equatorial osmium atom. The presence of a hydride bridging an equatorial-equatorial Os–Os bond introduces the electron imbalance, and requires an equatorial-apical Os–Os donor bond to restore the electron balance.

Depending on the structure of **7** (structure **A** or **B**, Fig. 1), the decarbonylation of **7** to **9** could involve either (i) a simple metal–metal bond formation, (ii) a metal framework rearrangement, or (iii) a ligand migration. If structure **B** is regarded as

Table 3

Bond angles (deg.) for $H_2Os_5(CO)_{13}P(OMe)_3PEt_3$ (**9**)

Os(2)–Os(1)–Os(3)	59.1(1)	Os(2)–Os(1)–Os(4)	59.3(1)
Os(3)–Os(1)–Os(4)	60.9(1)	Os(2)–Os(1)–P(1)	156.1(2)
Os(3)–Os(1)–P(1)	99.0(1)	Os(4)–Os(1)–P(1)	103.0(2)
Os(2)–Os(1)–C(11)	108.8(7)	Os(3)–Os(1)–C(11)	167.8(7)
Os(4)–Os(1)–C(11)	113.1(9)	P(1)–Os(1)–C(11)	92.6(6)
Os(2)–Os(1)–C(12)	102.0(5)	Os(3)–Os(1)–C(12)	94.2(5)
Os(4)–Os(1)–C(12)	153.7(5)	P(1)–Os(1)–C(12)	88.3(5)
C(11)–Os(1)–C(12)	89.7(10)	Os(1)–Os(2)–Os(3)	58.5(1)
Os(1)–Os(2)–Os(4)	54.9(1)	Os(3)–Os(2)–Os(4)	59.2(1)
Os(1)–Os(2)–Os(5)	101.1(1)	Os(3)–Os(2)–Os(5)	57.2(1)
Os(4)–Os(2)–Os(5)	55.5(1)	Os(1)–Os(2)–P(2)	144.0(2)
Os(3)–Os(2)–P(2)	112.5(1)	Os(4)–Os(2)–P(2)	155.5(2)
Os(5)–Os(2)–P(2)	100.2(1)	Os(1)–Os(2)–C(21)	64.9(7)
Os(3)–Os(2)–C(21)	106.0(7)	Os(4)–Os(2)–C(21)	116.2(7)
Os(5)–Os(2)–C(21)	163.1(7)	P(2)–Os(2)–C(21)	87.9(7)
Os(1)–Os(2)–C(22)	104.7(6)	Os(3)–Os(2)–C(22)	146.9(6)
Os(4)–Os(2)–C(22)	87.8(6)	Os(5)–Os(2)–C(22)	105.0(7)
P(2)–Os(2)–C(22)	97.3(6)	C(21)–Os(2)–C(22)	88.5(10)
Os(1)–Os(3)–Os(2)	62.3(1)	Os(1)–Os(3)–Os(4)	56.1(1)
Os(2)–Os(3)–Os(4)	59.1(1)	Os(1)–Os(3)–Os(5)	109.0(1)
Os(2)–Os(3)–Os(5)	64.0(1)	Os(4)–Os(3)–Os(5)	57.7(1)
Os(1)–Os(3)–C(31)	100.9(6)	Os(2)–Os(3)–C(31)	145.8(6)
Os(4)–Os(3)–C(31)	86.7(6)	Os(5)–Os(3)–C(31)	98.3(7)
Os(1)–Os(3)–C(32)	80.2(5)	Os(2)–Os(3)–C(32)	109.5(5)
Os(4)–Os(3)–C(32)	135.7(5)	Os(5)–Os(3)–C(32)	161.6(5)
C(31)–Os(3)–C(32)	95.3(9)	Os(1)–Os(3)–C(33)	162.6(7)
Os(2)–Os(3)–C(33)	109.0(5)	Os(4)–Os(3)–C(33)	134.7(7)
Os(5)–Os(3)–C(33)	77.5(7)	C(31)–Os(3)–C(33)	93.9(8)
C(32)–Os(3)–C(33)	89.4(9)	Os(1)–Os(4)–Os(2)	65.7(1)
Os(1)–Os(4)–Os(3)	63.0(1)	Os(2)–Os(4)–Os(3)	61.8(1)
Os(1)–Os(4)–Os(5)	118.6(1)	Os(2)–Os(4)–Os(5)	66.4(1)
Os(3)–Os(4)–Os(5)	61.6(1)	Os(1)–Os(4)–C(41)	113.8(8)
Os(2)–Os(4)–C(41)	157.6(6)	Os(3)–Os(4)–C(41)	97.4(7)
Os(5)–Os(4)–C(41)	97.5(6)	Os(1)–Os(4)–C(42)	68.4(10)
Os(2)–Os(4)–C(42)	109.0(8)	Os(3)–Os(4)–C(42)	129.6(10)
Os(5)–Os(4)–C(42)	165.6(8)	C(41)–Os(4)–C(42)	90.2(9)
Os(1)–Os(4)–C(43)	142.0(7)	Os(2)–Os(4)–C(43)	96.5(6)
Os(3)–Os(4)–C(43)	139.5(6)	Os(5)–Os(4)–C(43)	78.7(6)
C(41)–Os(4)–C(43)	95.2(10)	C(42)–Os(4)–C(43)	88.5(11)
Os(2)–Os(5)–Os(3)	58.8(1)	Os(2)–Os(5)–Os(4)	58.1(1)
Os(3)–Os(5)–Os(4)	60.7(1)	Os(2)–Os(5)–C(51)	143.4(7)
Os(3)–Os(5)–C(51)	88.6(7)	Os(4)–Os(5)–C(51)	92.9(6)
Os(2)–Os(5)–C(52)	108.3(8)	Os(3)–Os(5)–C(52)	103.2(8)
Os(4)–Os(5)–C(52)	162.3(8)	C(51)–Os(5)–C(52)	94.1(9)
Os(2)–Os(5)–C(53)	114.5(5)	Os(3)–Os(5)–C(53)	166.8(5)
Os(4)–Os(5)–C(53)	106.1(5)	C(51)–Os(5)–C(53)	93.6(9)
C(52)–Os(5)–C(53)	89.7(9)	Os(1)–P(1)–O(1)	119.1(10)
Os(1)–P(1)–O(2)	114.8(8)	Os(1)–P(1)–O(2)	105.7(13)
Os(1)–P(1)–O(3)	111.1(8)	O(1)–P(1)–O(3)	100.9(12)
O(2)–P(1)–O(3)	103.3(13)	P(1)–O(1)–C(1)	131.0(25)
P(1)–O(2)–C(2)	138.4(23)	P(1)–O(3)–C(3)	136.6(23)
Os(2)–P(2)–C(4)	112.5(9)	Os(2)–P(2)–C(6)	114.9(7)
C(4)–P(2)–C(6)	106.1(11)	Os(2)–P(2)–C(8)	114.2(8)
C(4)–P(2)–C(8)	103.5(12)	C(6)–P(2)–C(8)	104.8(13)

(continued)

Table 3 (continued)

P(2)–C(4)–C(5)	116.6(22)	P(2)–C(6)–C(7)	113.8(21)
P(2)–C(8)–C(9)	114.5(21)	Os(1)–C(11)–O(11)	177.7(24)
Os(1)–C(12)–O(12)	176.8(14)	Os(2)–C(21)–O(21)	166.3(21)
Os(2)–C(22)–O(22)	173.4(18)	Os(3)–C(31)–O(31)	176.1(21)
Os(3)–C(32)–O(32)	174.3(14)	Os(3)–C(33)–O(33)	170.2(18)
Os(4)–C(41)–O(41)	178.1(21)	Os(4)–C(42)–O(42)	166.6(26)
Os(4)–C(43)–O(43)	171.9(21)	Os(5)–C(51)–O(51)	175.9(20)
Os(5)–C(52)–O(52)	178.0(16)	Os(5)–C(53)–O(53)	177.8(17)

the correct structure of **7**, then the decarbonylation would simply involve a metal–metal bond formation to give **9** (Fig. 2). If structure **A** is the actual structure for **7**, then the decarbonylation would involve either a metal framework rearrangement or ligand migration, or perhaps both. Keeping these ideas in mind, we monitored the decarbonylation of **7** by ^{1}H NMR spectroscopy. On the NMR time scale no dissociation of the phosphite/phosphine ligand was detected, which minimises the possibility of migration of the ligand from one osmium atom to another. Thus the transformation of **7** (structure **A**) to **9** is thought to involve a metal polyhedron rearrangement (Fig. 6). The metal polyhedron rearrangement shown in Fig. 6 proceeds via a square-based pyramidal intermediate, which is an alternative geometry for a 74 electron cluster.

The chemical activation of the cluster $H_2Os_5(CO)_{14}L$ (L = $P(OMe)_3$ (**2**) or PEt_3 (**3**)) with Me_3NO in the presence of $P(OMe)_3$ affords $H_2Os_5(CO)_{13}LP(OMe)_3$ (L = $P(OMe)_3$ (**8**) or PEt_3 (**9**)) suggesting that a simple substitution of a carbonyl ligand by a ligand L is taking place. This is in contrast to the thermal activation, in which the substitution proceeds via formation of an addition product and involves metal skeleton rearrangement.

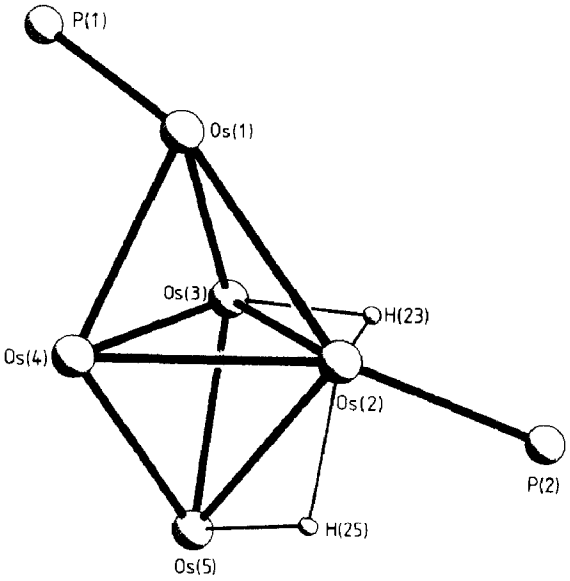

Fig. 5. The core geometry of $H_2Os_5(CO)_{13}P(OMe)_3PEt_3$ (**9**) showing the calculated positions of the two hydrides.

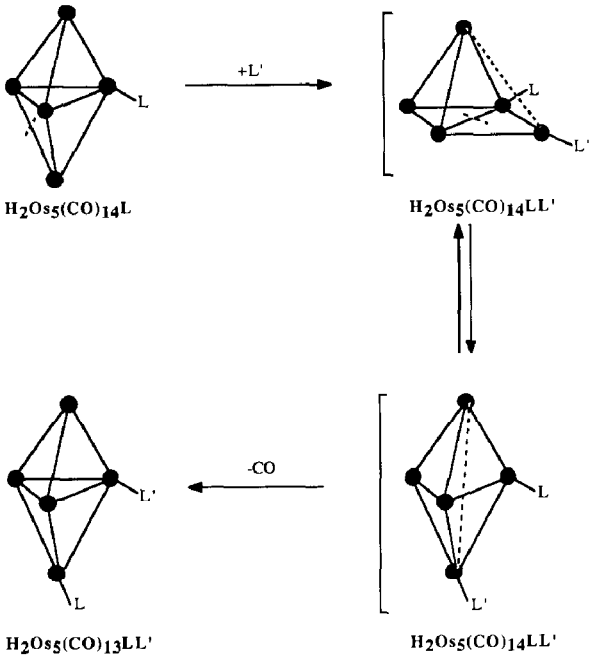

Fig. 6. Metal polyhedron rearrangement proposed for the decarbonylation of $H_2Os_5(CO)_{14}LL'$ (**7**) to $H_2Os_5(CO)_{13}LL'$ (**9**) (L = $P(OMe)_3$, L' = PEt_3).

Experimental

Although none of the clusters reported here is particularly air-sensitive, all the reactions, purifications, etc. were carried out under dinitrogen.

Proton and ^{31}P NMR spectra data were recorded on Bruker WM250 spectrometer at 20 °C using deuterated solvent as internal lock and reference (^1H: $SiMe_4$, δ 0; ^{31}P: 1%$P(OMe)_3$ in C_6D_6, δ 0; downfield positive). Infrared spectra were recorded on a Perkin Elmer 983 spectrometer and the mass spectra were obtained with an AEI MS12 spectrometer with ca. 70 eV (1.12×10^{-17} J) ionizing potential at 100–150 °C. Tris(perfluoroheptyl)-*s*-triazine was used as reference.

The compounds $H_2Os_5(CO)_{15}$ [8,9] and $H_2Os_5(CO)_{14}L$ [2,4] (L = $P(OMe)_3$ or PEt_3) were prepared by published methods. Trimethylamine-*N*-oxide was freshly sublimed before use. All the other reagents were commercial grade, and used as obtained.

*Preparation of $H_2Os_5(CO)_{14}P(OMe)_3L$ (L = $P(OMe)_3$ (**6**) or PEt_3 (**7**))*

A solution of $H_2Os_5(CO)_{14}P(OMe)_3$ (**2**) and an excess of the ligand L (L = $P(OMe)_3$ or PEt_3) in toluene was kept at 80 °C for 6 h. The solvent and excess of ligand were then removed on a fast stream of N_2. Separation of the mixture by TLC gave the brown cluster $H_2Os_5(CO)_{14}P(OMe)_3L$ (L = $P(OMe)_3$ (**6**) or PEt_3 (**7**)) in 60% yield.

*Decarbonylation of $H_2Os_5(CO)_{14}P(OMe)_3L$ (L = $P(OMe)_3$ (**6**) or PEt_3 (**7**))*

A solution of $H_2Os_5(CO)_{14}P(OMe)_3L$ (L = $P(OMe)_3$ (**6**) or PEt_3 (**7**)) in toluene was kept at 80 °C for 6 h. Removal of solvent under pressure followed by TLC yielded $H_2Os_5(CO)_{13}P(OMe)_3L$ (L = $P(OMe)_3$ (**8**) or PEt_3 (**9**)) in 80% yield.

Carbonylation of $H_2Os_5(CO)_{13}P(OMe)_3L$ (L = $P(OMe)_3$ (8) or PEt_3 (9))

A solution of $H_2Os_5(CO)_{13}P(OMe)_3L$ (L = $P(OMe)_3$ (**8**) or PEt_3 (**9**)) in toluene was placed in a Roth autoclave, which was then charged with 40 atm of CO and kept at 50 °C for 4 h. Work up by chromatography gave $H_2Os_5(CO)_{14}P(OMe)_3L$ (L = $P(OMe)_3$ (**6**) or PEt_3 (**7**)) in 70% yield.

Preparation of $H_2Os_5(CO)_{13}\{P(OMe)_3\}_2$ (8)

A solution of $H_2Os_5(CO)_{14}P(OMe)_3$ (**2**) and an excess of $P(OMe)_3$ in n-heptane was refluxed for 5 h. The solvent was then removed under pressure and the residue subjected to TLC to give $H_2Os_5(CO)_{13}\{P(OMe)_3\}_2$ (**8**) as the major product.

Preparation of $H_2Os_5(CO)_{13}P(OMe)_3PEt_3$ (9)

A solution of $H_2Os_5(CO)_{14}P(OMe)_3$ (**2**) and an excess of PEt_3 in n-heptane was refluxed for 16 h. Work up by chromatography gave $H_2Os_5(CO)_{13}P(OMe)_3PEt_3$ (**9**) in 80% yield.

Reaction of $H_2Os_5(CO)_{14}P(OMe)_3$ (L = $P(OMe)_3$ (2) or PEt_3 (3)) with Me_3NO/$P(OMe)_3$

A solution of $H_2Os_5(CO)_{14}L$ (L = $P(OMe)_3$ (**2**) or PEt_3 (**3**)) (30 mg) and an excess of $P(OMe)_3$ in CH_2Cl_2 (25 cm^3) was stirred in $P(OMe)_3$. A solution of Me_3NO (1.1 eq. in 20 cm^3 CH_2Cl_2) was then added dropwise to the stirred suspension at −78 °C during 0.5 h. The mixture was allowed to warm slowly to room temperature and stirred for another 0.5 h. The solvent and the excess of ligand were then removed in a fast stream of N_2. Work up by TLC (50% CH_2Cl_2 in hexane) gave $H_2Os_5(CO)_{13}LP(OMe)_3$ (L = $P(OMe)_3$ (**8**) or PEt_3 (**9**)) in 50–60% yield.

Crystal structure determination of $H_2Os_5(CO)_{13}P(OMe_3)PEt_3$ (9)

Suitable single crystals were obtained as red platelets from CH_2Cl_2/hexane solution at −5 °C. A crystal with dimensions (distance from face to centre): 0.034 (1 0 0, −1 0 0) × 0.095 (0 0 1, 0 0 − 1) × 0.154 (0 1 0, 0 − 1 0) mm was mounted on a glass fibre with epoxy resin.

Crystal data. $C_{22}H_{26}O_{16}Os_5P_2$, M = 1559.4, Monoclinic, a 17.966 (3), b 11.564 (2), c 18.080(2) Å, β 112.85 (1)°, V 3461.5 Å^3 (by least-squares fit for 68 automatically centred reflections in the range $15 < 2\theta < 25°$), space group $P2_1/c$ (No. 14), Z = 4, D_c 2.99 g cm^{-3}, F (000) = 2784, graphite monochromated Mo-K_α radiation, λ 0.71069 Å, μ (Mo-K_α) 184.30 cm^{-1}.

Data collection and processing. Stoe STADI-4 diffractometer, 24 step ω–θ scan with scan width 0.04°, scan time 0.5–3.0 s per step; 6648 reflections measured ($5.0 < 2\theta < 50.0°$, $+h$, $-k$, $\pm l$), (6099 unique, merging R = 0.049 after empirical absorption correction based on an ellipsoid model and 300 azimuthal scan data (max. and min. transmission factors 0.116, 0.035), giving 4607 unique with $F > 4\sigma(F)$. Three standard reflections showed no significant variation in intensity.

Structure analysis and refinement. Centrosymmetric direct methods (Os atoms) followed by Fourier difference techniques for remaining non-hydrogen atoms. Blocked cascade least-squares with Os, P, O, and carbonyl C atoms anisotropic. The phosphine and phosphite H-atoms were placed in calculated positions (C–H 1.08 Å) and allowed to ride on the relevant C atoms; the temperature factors for these

Table 4

Atom coordinates ($\times 10^4$) for $H_2Os_5(CO)_{13}P(OMe)_3PEt_3$ (9)

	x	y	z
Os(1)	2941(1)	5083(1)	4578(1)
Os(2)	3111(1)	3021(1)	5629(1)
Os(3)	1889(1)	3117(1)	4012(1)
Os(4)	1843(1)	4648(1)	5210(1)
Os(5)	1347(1)	2414(1)	5229(1)
P(1)	2297(4)	6322(5)	3584(3)
O(1)	1474(15)	6810(17)	3508(14)
C(1)	1281(28)	7798(33)	3755(24)
O(2)	2830(17)	7437(18)	3534(14)
C(2)	2813(30)	8304(34)	2967(26)
O(3)	2066(14)	5735(17)	2744(10)
C(3)	1546(21)	5942(30)	1988(19)
P(2)	3709(3)	1158(4)	5965(3)
C(4)	3301(16)	341(19)	6556(14)
C(5)	3731(18)	−836(24)	6907(16)
C(6)	4812(14)	1163(20)	6526(13)
C(7)	5070(18)	1610(24)	7367(16)
C(8)	3545(18)	222(22)	5097(15)
C(9)	3913(22)	643(31)	4550(20)
C(11)	3722(14)	6220(16)	5167(14)
O(11)	4161(11)	6909(12)	5518(10)
C(12)	3596(10)	4674(15)	4025(11)
O(12)	4039(10)	4422(14)	3712(9)
C(21)	4091(15)	3540(21)	5556(14)
O(21)	4731(9)	3687(16)	5630(10)
C(22)	3486(12)	3619(16)	6674(11)
O(22)	3646(10)	4040(15)	7292(8)
C(31)	876(14)	3883(18)	3276(11)
O(31)	355(10)	4255(15)	2861(8)
C(32)	2395(11)	3104(13)	3261(10)
O(32)	2648(13)	3032(23)	2776(11)
C(33)	1492(13)	1587(23)	3679(11)
O(33)	1216(12)	731(16)	3369(10)
C(41)	804(13)	5304(17)	4614(12)
O(41)	182(8)	5702(14)	4277(8)
C(42)	2273(15)	6098(21)	5471(14)
O(42)	2517(13)	7008(17)	5776(12)
C(43)	1712(14)	4607(16)	6205(14)
O(43)	1711(11)	4667(16)	6837(8)
C(51)	260(14)	2750(18)	4501(10)
O(51)	−376(9)	2987(16)	4111(9)
C(52)	1224(15)	778(22)	5078(12)
O(52)	1135(14)	−211(14)	4963(12)
C(53)	1064(12)	2293(15)	6135(12)
O(53)	866(10)	2221(15)	6667(8)

atoms were fixed. The weighting scheme $\omega^{-1} = \sigma^2(F) + 0.0008(F)^2$ gave satisfactory agreement analyses. The refinement converged at R and R_w values of 0.056 and 0.055. A final difference map showed ripples of ca. 2.4e $Å^{-3}$ close to Os atom positions. Complex neutral atom scattering factors were employed [10], and all

computations were performed on the University of Cambridge IBM 3084 Q computer using SHELX76 [11]. The final atomic fractional coordinates for the non-hydrogen atoms are presented in Table 4 *.

Acknowledgements

We thank the Nehru Trust, the Cambridge Commonwealth Trust, and the Committee of Vice-Chancellors and Principals for the financial support (to RK), the Universidad Nácional Autonoma de México for a grant (to MJR).

References

1 G.F. John, B.F.G. Johnson, J. Lewis, W.J.H. Nelson, and M. McPartlin, J. Organomet. Chem., 171 (1979) C14.
2 B.F.G. Johnson, J. Lewis, P.R. Raithby, and M.J. Rosales, J. Organomet. Chem., 259 (1983) C9.
3 D.H. Farrar, B.F.G. Johnson, J. Lewis, P.R. Raithby, and M.J. Rosales, J. Chem. Soc., Dalton Trans., (1982) 2051.
4 R. Khattar, B.F.G. Johnson, J. Lewis, P.R. Raithby, and M.J. Rosales, J. Chem. Soc., Dalton Trans., to be submitted.
5 L.J. Farrugia, M.J. Freeman, M. Green, A.G. Orpen, F.G.A. Stone, and I.D. Salter, J. Organomet. Chem., 249 (1983) 273.
6 M.J. Freeman, A.G. Orpen, and I.D. Salter, J. Chem. Soc., Dalton Trans., (1987) 379.
7 B.F.G. Johnson, J. Chem. Soc., Chem. Commun., (1986) 27.
8 C.R. Eady, J.J. Guy, B.F.G. Johnson, J. Lewis, M.L. Malatesta, and G.M. Sheldrick, J. Chem. Soc., Chem. Commun., (1976) 807.
9 J.N. Nicholls and M.D. Vargas, Inorg. Syntheses, in press.
10 International tables for X-ray Crystallography, Kynoch Press, Birmingham, 1974, Vol. 4.
11 SHELX 76, Crystal Structure Solving Package, G.M. Sheldrick, Cambridge, 1976.

* Thermal parameters, complete lists of bond parameters and hydrogen atom positions, and lists of structure factors may be obtained from the authors.